Volume 1 | Number 1 | Jan 2013 | Pages 1–100

ChemComm

Chemical Communications
www.rsc.org/chemcomm

ROYAL SOCIETY OF CHEMISTRY

This is an *Accepted Manuscript*, which has been through the Royal Society of Chemistry peer review process and has been accepted for publication.

Accepted Manuscripts are published online shortly after acceptance, before technical editing, formatting and proof reading. Using this free service, authors can make their results available to the community, in citable form, before we publish the edited article. We will replace this *Accepted Manuscript* with the edited and formatted *Advance Article* as soon as it is available.

You can find more information about *Accepted Manuscripts* in the **Information for Authors**.

Please note that technical editing may introduce minor changes to the text and/or graphics, which may alter content. The journal's standard **Terms & Conditions** and the **Ethical guidelines** still apply. In no event shall the Royal Society of Chemistry be held responsible for any errors or omissions in this *Accepted Manuscript* or any consequences arising from the use of any information it contains.

www.rsc.org/chemcomm

Journal Name

Dynamic Article Links ▶

ARTICLE TYPE

Formation of polyphenyl chains through hierarchical reactions: Ullmann coupling followed by cross-dehydrogenative coupling

Chi Zhang, Qiang Sun, Hua Chen, Qinggang Tan, and Wei Xu*

From an interplay of UHV-STM imaging and DFT calculations, we have illustrated on-surface formation of polyphenyl chains through a hierarchical reaction pathway involving two different kinds of reactions (Ullmann coupling
10 **and cross-dehydrogenative coupling), which will provide deeper understandings of on-surface chemical reactions and an alternative and efficient strategy to fabricate desired surface molecular nanostructures.**
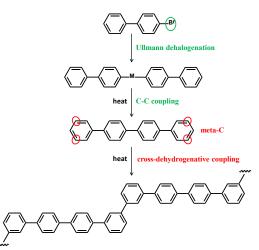
One urgent pursuit of the continuously developing nanoscience
15 and nanotechnology is to achieve robust nanostructures by using the bottom-up strategy. Construction of covalently interlinked molecular nanostructures with relatively high thermal stability[1] and efficient intermolecular charge transport[2,3] has demonstrated to be a promising method for further applications within the field
20 of nanotechnology, e.g. molecular nanoelectronics and nanospintronics. Recently, several typical chemical reactions have been extensively employed and successfully introduced from solution to various metal surfaces within the surface science community, such as Ullmann coupling[4-18], Bergman
25 cyclization[19,20], Glaser coupling[21,22], click reaction[23]. Furthermore, it has also been demonstrated that specific metal substrates may facilitate some unexpected reactions which can hardly take place in solution, such as surface-catalyzed cyclodehydrogenation[24], C-C coupling of alkane molecules[25] and intermolecular cross-
30 dehydrogenative coupling[26]. However, to our knowledge, on-surface fabrication of nanostructures has been mainly through one-step reactions[19-29] or one kind of reaction in a hierarchical manner[5,14]. Thus, it would be of utmost interest to explore the feasibility of inducing on-surface hierarchical reactions involving
35 different kinds of chemical reactions[6] with distinct characteristics such as reaction temperatures and/or appropriate reactive sites, which is particularly crucial for delicate fabrications of more sophisticated surface nanostructures.

In this work, we choose the 4-bromobiphenyl (shortened as
40 BBP) molecule as the precursor which contains one halogen atom (i.e. Br) capable of introducing Ullmann coupling, and the meta-carbon sites (cf. Scheme 1) that can undergo cross-dehydrogenative coupling via C-H activation[26]. It is known that the Ullmann dehalogenation can take place at relatively low
45 temperatures (typically between 170 K and 240 K) on the copper surface[7-13], and the subsequent cross-dehydrogenative coupling would take place at higher temperatures (~500 K)[26], which allows us to explore the possible hierarchical reactions on the surface

50 Scheme 1. Schematic illustration on the reaction path of forming polyphenyl chains via hierarchical chemical reactions (i.e. Ullmann dehalogenation and C-C coupling and subsequent cross-dehydrogenative coupling). M denotes a metal atom.

under ultrahigh vacuum (UHV) conditions. From the interplay of
55 high-resolution scanning tunneling microscopy (STM) imaging and density functional theory (DFT) calculations, we have demonstrated that on a Cu(110) surface the BBP molecules dehalogenate and form the corresponding organometallic intermediate at RT. Subsequent thermal treatment (~465 K)
60 releases the linking metal atoms and consequently the quaterphenyl (shortened as (Ph)$_4$) molecules are formed as the product of Ullmann coupling. As expected, still interestingly, further thermal treatment at even higher temperatures (~500 K) results in the formation of covalently bound polyphenyl chains
65 based on (Ph)$_4$ molecules via cross-dehydrogenative coupling. We have, thus, demonstrated the feasibility of fabrication of covalently interlinked nanostructures through on-surface hierarchical chemical reactions as outlined in Scheme 1. These findings will help us to gain deeper insight into fundamental
70 understandings of on-surface chemical reactions, and may present an alternative and efficient strategy to fabricate more sophisticated surface molecular nanostructures with further applications in molecular nanoelectronics and so on.

Deposition of BBP molecules on Cu(110) held at RT leads to
75 the formation of ordered networks composed of rod-like structures surrounded with bright dots as shown in Figure 1a and1b. Close inspection enables us to indentify that the rod-like
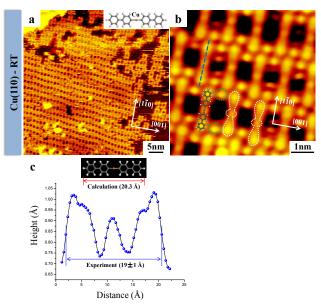
Figure 1. Formation of organometallic intermediate on Cu(110). (a) The large-scale STM image showing the formation of a porous network composed of $(Ph)_2$-Cu-$(Ph)_2$ intermediates and detached Br atoms after deposition of BBP molecules on Cu(110) held at RT. The upper right inset showing the chemical structure of the formed $(Ph)_2$-Cu-$(Ph)_2$ organometallic intermediate where C is gray, H is white and Cu is brown. (b) The close-up STM image showing the details of the organometallic intermediate with the scaled gas-phase optimized structural model superimposed. The green ovals indicate the detached Br atoms, and the white contours indicate the organometallic intermediates. Scanning conditions: $I_t = 1.10$ nA, $V_t = -1500$ mV. (c) The line-scan profile along the blue dashed line in (b). The upper panel showing the gas-phase optimized structural model of $(Ph)_2$-Cu-$(Ph)_2$ intermediate.

structures tend to mainly array along the $[1\bar{1}0]$ direction of the substrate, and each one is imaged as two lobes and a bright protrusion in the center that are attributed to the biphenyl groups and the Cu atom[7-13], respectively. Similar structures have been widely reported and proved to be organometallic intermediates[7-13] in Ullmann coupling process. In addition, the isolated bright dots (indicated by the green ovals in Figure 1b) are attributed to the detached Br atoms as also found in the previous studies[7-13]. Moreover, the length of the $(Ph)_2$-Cu-$(Ph)_2$ intermediate is measured to be 19±1 Å from the line-scan profile as illustrated in Figure 1c, which is in accordance with the theoretical value (20.3 Å). The scaled theoretical model is also superimposed on an individual intermediate where good agreement is achieved. Thus, deposition of BBP molecule on Cu(110) held at RT results in the C–Br bond dissociation and the formation of organometallic intermediate.
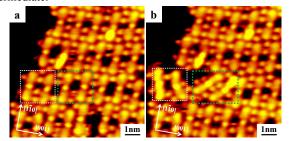

Figure 2. Lateral STM manipulation on the organometallic intermediates on Cu(110). The white rectangles and green rectangles in (a) and (b) highlight the twist of the C-Cu bond and the local translation before and after manipulation, respectively.
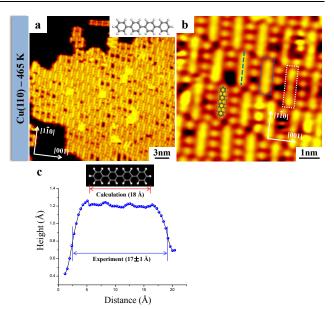

Figure 3. Formation of $(Ph)_4$ molecule after subsequent thermal treatment on Cu(110). (a) The large-scale STM image showing the formation of a close-packed structure composed of the newly formed $(Ph)_4$ molecules and the remaining $(Ph)_2$-Cu-$(Ph)_2$ intermediates after annealing the Cu(110) sample to ~465 K. The upper right inset showing the chemical structure of $(Ph)_4$. (b) The close-up STM image showing the details of the $(Ph)_4$ molecule with the scaled gas-phase optimized structural model superimposed. The blue and white rectangles indicate the $(Ph)_4$ and $(Ph)_2$-Cu-$(Ph)_2$, respectively. Scanning conditions: $I_t = 0.89$ nA, $V_t = -1200$ mV. (c) The line-scan profile along the blue dashed line in (b). The upper panel showing the gas-phase optimized structural model of $(Ph)_4$.

To test the robustness of the formed organometallic intermediate, we have performed lateral STM manipulations as shown in Figure 2. After disturbed by the STM tip (parameters: $I_t = 5.10$ nA, $V_t = -20$ mV), the $(Ph)_2$-Cu-$(Ph)_2$ intermediates either change the initial morphology with the C-Cu bond twisted or translate with a different molecular orientation as indicated by white rectangles and green rectangles, respectively, which indicates the relative robustness of the C-Cu bonding and the flexibility of the C-Cu-C bond.

Subsequent annealing the Cu(110) sample to 465 K results in the formation of a similar close-packed nanostructure with rod-like molecules still arraying along the $[1\bar{1}0]$ direction of the substrate (Figure 3a). From the close-up STM image (Figure 3b), we can clearly distinguish two different kinds of rod-like features coexisting on the surface. Besides some remaining $(Ph)_2$-Cu-$(Ph)_2$ intermediates (one of them is indicated by the white rectangle), the newly formed shorter rods with uniform intramolecular brightness are also found (one of them is indicated by the blue rectangle), which are naturally attributed to the $(Ph)_4$ molecules based on the Ullmann C-C coupling scenario. The length of the formed $(Ph)_4$ molecule is measured to be 17±1 Å from the line-scan profile as illustrated in Figure 3c, which is in accordance with the theoretical result (18 Å), and also well matches the dimension and morphology of $(Ph)_4$ molecule on Cu(110) reported in the previous work[26]. The scaled gas-phase optimized model is also superimposed on the STM image and good agreement is achieved. It is noticed that in this structure more bright dots surrounding the $(Ph)_4$ and $(Ph)_2$-Cu-$(Ph)_2$ are found, which should be attributed to the released Cu atoms besides the Br atoms. Also note that the $(Ph)_2$-Cu-$(Ph)_2$ intermediates coexist
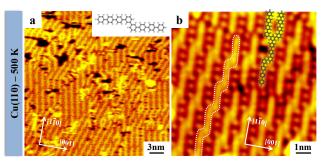
Figure 4. Formation of polyphenyl chains on Cu(110) after further thermal treatment at a higher temperature. (a) The large-scale STM image showing the formation of polyphenyl chains after further annealing the Cu(110) sample to 500 K. The upper right inset showing the chemical structure of a simplified polyphenyl chain. (b) The close-up STM image showing the details of the polyphenyl chains with the structural model superimposed. The white contour depicts a polyphenyl chain. Scanning conditions: I_t = 1.20 nA, V_t = -2000 mV.

with $(Ph)_4$ molecules in a wide temperature window ranging from 440 K to 470 K, and higher temperatures lead to the additional reactions which will be discussed below. Thus, annealing the Cu(110) sample to ~465 K results in the C–Cu bond dissociation and the formation of $(Ph)_4$ product from Ullmann coupling.

Further annealing the Cu(110) sample to 500 K, as expected, still interestingly, we find the formation of separated molecular chains (Figure 4a). The close-up STM image (Figure 4b) shows the details of the chain structures (one of them is indicated by the white contour) in which we identify that the dimension and morphology of each unit and the covalent C-C interlinking are identical and also consistent with that of $(Ph)_4$ molecule and each unit binds with each other in a shoulder-to-shoulder mode with the same characteristics of polyphenyl chains formed by $(Ph)_4$ on Cu(110) reported previously[26]. The comparison of the theoretical models of direct C-C coupling and C-Cu-C interlinking indicates a good agreement between the direct C-C coupling and the experimental lateral offset of the polyphenyl chain (Figure S1). Similar previous works of cross-dehydrogenative coupling on metal surfaces in UHV have also been reported[25,29]. Also note that the activation temperature in this step (~500 K) is exactly when cross-dehydrogenative coupling of $(Ph)4$ on Cu(110) takes place[26]. Thus we believe that the chains shown in Figure 4a and b are the target polyphenyl chains resulting from $(Ph)_4$ molecules (the products of the cross-dehydrogenative coupling via C-H activation at the meta-C sites as reported in our previous work[26]). Note that due to the coexistence of Br atoms in between, the polyphenyl chains tend to be quasilinear and have fewer branches in comparison with that of direct cross-dehydrogenative coupling of $(Ph)_4$[26]. The model of chain and branch structures is also superimposed on the STM image. Further annealing the polyphenyl chains on Cu(110) to 525 K results in the disordered chains with Br atoms surrounded as shown in Figure S2.

To extend the studied system we have also investigate the behaviors of BBP molecule on a Ag(110) surface. Similar to the situation on Cu(110), deposition of BBP molecules on Ag(110) held at RT results in the formation of $(Ph)_2$-Ag-$(Ph)_2$ organometallic intermediates surrounded with detached Br atoms (Figure 5a and 5b), which is also consistent with previous studies on silver surface[14-18]. On Ag(110) the $(Ph)_2$-Ag-$(Ph)_2$ intermediates array in different directions as shown in Figure 5a.
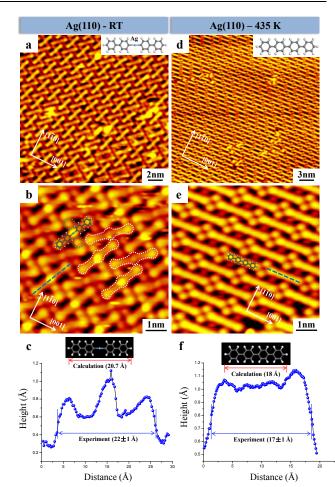

Figure 5. Formation of $(Ph)_2$-Ag-$(Ph)_2$ organometallic intermediate and $(Ph)_4$ molecule on Ag(110). (a) and (d) The large-scale STM images showing the formation of close-packed nanostructures composed of $(Ph)_2$-Ag-$(Ph)_2$ intermediates after deposition of BBP molecules on Ag(110) held at RT and $(Ph)_4$ molecules after further annealing the sample to ~435 K, respectively. The upper right insets showing the chemical structures of the formed $(Ph)_2$-Ag-$(Ph)_2$ intermediate and the $(Ph)_4$ molecule, respectively, where C is gray, H is white and Ag is azure. (b) and (e) The close-up STM images showing the details of the $(Ph)_2$-Ag-$(Ph)_2$ intermediates and $(Ph)_4$ molecules with the scaled gas-phase optimized structural models superimposed, respectively. The green ovals in (b) indicate the detached Br atoms, and the white contours indicate the organometallic intermediates. Scanning conditions: I_t = 1.00 nA, V_t = -1300 mV. (c) and (f) The line-scan profiles along the blue dashed lines in (b) and (e), respectively. The upper panels showing the gas-phase optimized structural models of the $(Ph)_2$-Ag-$(Ph)_2$ intermediate and the $(Ph)_4$ molecule, respectively.

Annealing the sample to ~435 K leads to the formation of $(Ph)_4$ molecules completely which mainly array along the [001] direction of the substrate with Br atoms surrounded (Figure 5d and 5e). The scaled gas-phase optimized structural models of $(Ph)_2$-Ag-$(Ph)_2$ and $(Ph)_4$ are superimposed on the close-up STM images with good agreements, respectively. The lengths of the $(Ph)_2$-Ag-$(Ph)_2$ intermediate and $(Ph)_4$ molecule are measured to be 20±1 Å and 17±1 Å from the line-scan profiles as illustrated in Figure 5c and f, which are in accordance with the theoretical values of 20.3 Å and 18 Å, respectively. Further annealing the sample to the temperature window ranging from 500 K to 525 K, however, does not result in the formation of ordered polyphenylchains as found on Cu(110), and instead some disordered short chains are formed (Figure S3). In the disordered chain structures, each unit links to another one with smooth and

ChemComm Accepted Manuscript

identical junctions and a specific angle which may be attributed to a certain reaction. From that we conclude the final step of the hierarchical reaction (i.e. cross-dehydrogenative coupling via C-H activation at the meta-C sites) can only be realized on Cu(110) and not on Ag(110). As we know the orientation of the formed $(Ph)_4$ molecules on Cu(110) (i.e. along the $[1\bar{1}0]$ direction) and the corresponding registry with respect to the substrate facilitate the cross-dehydrogenative coupling at the meta-C sites[26]. With respect to the case on Ag(110): (1) The formed $(Ph)_4$ molecules have a different molecular orientation (i.e. along the [001] direction) and thus different registry with respect to the substrate; (2) The detached Br atoms are distributed in-between the two terminals of the $(Ph)_4$ molecules, which may hamper the C-H activation at the meta-C sites. (3) The intrinsically different chemical nature of the surface compared with Cu(110).

In conclusion, from an interplay of UHV-STM imaging and DFT calculations, we have illustrated on-surface formation of polyphenyl chains through a hierarchical reaction pathway involving two different kinds of reactions, that is, Ullmann coupling and cross-dehydrogenative coupling. The studied system may not only serve as a simple and practical route for multifold fabrication of surface molecular nanostructures, but also provide the possibility of exploring more sophisticated on-surface chemical reactions.

Notes and references

Tongji-Aarhus Joint Research Center for Nanostructures and Functional Nanomaterials and College of Materials Science and Engineering, Tongji University, Caoan Road 4800, Shanghai 201804, P. R. China
E-mail: xuwei@tongji.edu.cn
† Electronic Supplementary Information (ESI) available: [The experimental and computational methods and STM images]. See DOI: 10.1039/b000000x/

1 A. P. Cote, A. I. Benin, N. W. Ockwig, M. O'Keeffe, A. J. Matzger and O. M. Yaghi, *Science*, 2005, **310**, 1166.

2 S. Wan, F. Gándara, A. Asano, H. Furukawa, A. Saeki, S. K. Dey, L. Liao, M. W. Ambrogio, Y. Y. Botros, X. Duan, S. Seki, J. F. Stoddart and O. M. Yaghi, *Chem. Mater.*, 2011, **23**, 4094.

3 A. Nitzan and M. A. Ratner, *Science*, 2003, **300**, 1384.

4 L. Grill, M. Dyer, L. Lafferentz, M. Persson, M. V. Peters and S. Hecht, *Nature Nanotech.*, 2007, **2**, 687.

5 L. Lafferentz, V. Eberhardt, C. Dri, C. Africh, G. Comelli, F. Esch, S. Hecht and L. Grill, *Nat. Chem.*, 2012, **4**, 215.

6 J. Cai, P. Ruffieux, R. Jaafar, M. Bieri, T. Braun, S. Blankenburg, M. Muoth, A. P. Seitsonen, M. Saleh, X. Feng, K. Müllen and R. Fasel, *Nature*, 2010, **466**, 470.

7 Q. Fan, C. Wang, Y. Han, J. Zhu, W. Hieringer, J. Kuttner, G. Hilt and J. M. Gottfried, *Angew. Chem. Int. Ed.*, 2013, **52**, 4668.

8 W. Wang, X. Shi, S. Wang, M. A. Van Hove and N. Lin, *J. Am. Chem. Soc.*, 2011, **133**, 13264.

9 E. A. Lewis, C. J. Murphy, M. L. Liriano and E. C. H. Sykes, *Chem. Commun.*, 2014, **50**, 1006.

10 H. Walch, R. Gutzler, T. Sirtl, G. Eder and M. Lackinger, *J. Phys. Chem. C*, 2010, **114**, 12604.

11 Q. Fan, C. Wang, L. Liu, Y. Han, J. Zhao, J. Zhu, J. Kuttner, G. Hilt and J. M. Gottfried, *J. Phys. Chem. C*, 2014, **118**, 13018.

12 M. Koch, M. Gille, A. Viertel, S. Hecht and L. Grill, *Surf. Sci.*, 2014, **627**, 70.

13 M. Chen, J. Xiao, H. P. Steinrück, S. Wang, W. Wang, N. Lin, W. Hieringer and J. M. Gottfried, *J. Phys. Chem. C*, 2014, 118, 6820.

14 J. Eichhorn, T. Strunskus, A. Rastgoo-Lahrood, D. Samanta, M. Schmittel and M. Lackinger, *Chem. Commun.*, 2014, **50**, 7680.

15 M. Bieri, S. Blankenburg, M. Kivala, C. A. Pignedoli, P. Ruffieux, K. Müllen and R. Fasel, *Chem. Commun.*, 2011, **47**, 10239.

16 J. Park, K. Y. Kim, K. H. Chung, J. K. Yoon, H. Kim, S. Han and S. J. Kahng, *J. Phys. Chem. C*, 2011, **115**, 14834.

17 K. H. Chung, B. G. Koo, H. Kim, J. K. Yoon, J. H. Kim, Y. K. Kwon and S. J. Kahng, *Phys. Chem. Chem. Phys.*, 2012, **14**, 7304.

18 L. Cardenas, R. Gutzler, J. Lipton-Duffin, C. Fu, J. L. Brusso, L. E. Dinca, M. Vondráček, Y. Fagot-Revurat, D. Malterre, F. Rosei and D. F. Perepichka, *Chem. Sci.*, 2013, **4**, 3263.

19 Q. Sun, C. Zhang, Z. Li, H. Kong, Q. Tan, A. Hu and W. Xu, *J. Am. Chem. Soc.*, 2013, **135**, 8448.

20 A. Riss, S. Wickenburg, P. Gorman, L. Z. Tan, H. Z. Tsai, D. G. de Oteyza, Y. C. Chen, A. J. Bradley, M. M. Ugeda, G. Etkin, S. G. Louie, F. R. Fischer and M. F. Crommie. *Nano Lett.*, 2014, **14**, 2251.

21 H. Y. Gao, H. Wagner, D. Zhong, J. H. Franke, A. Studer and H. Fuchs, *Angew. Chem. Int. Ed.*, 2013, **52**, 4024.

22 Y. Q. Zhang, N. Kepčija, M. Kleinschrodt, K. Diller, S. Fischer, A. C. Papageorgiou, F. Allegretti, J. Björk, S. Klyatskaya, F. Klappenberger, M. Ruben and J. V. Barth, *Nat. Commun.*, 2012, **3**, 1286.

23 F. Bebensee, C. Bombis, S. R. Vadapoo, J. R. Cramer, F. Besenbacher, K. V. Gothelf, T. R. Linderoth, *J. Am. Chem. Soc.*, 2013, **135**, 2136.

24 G. Otero, G. Biddau, C. Sánchez-Sánchez, R. Caillard, M. F. López, C. Rogero, F. J. Palomares, N. Cabello, M. A. Basanta, J. Ortega, J. Méndez, A. M. Echavarren, R. Pérez, B. Gómez-Lor and J. A. Martín-Gago, *Nature*, 2008, **454**, 865.

25 D. Zhong, J. H. Franke, S. K. Podiyanachari, T. Blömker, H. Zhang, G. Kehr, G. Erker, H. Fuchs and L. Chi, *Science*, 2011, **334**, 213.

26 Q. Sun, C. Zhang, H. Kong, Q. Tan and W. Xu, *Chem. Commun.*, 2014, **50**, 11825.

27 M. Treier, N. V. Richardson and R. Fasel, *J. Am. Chem. Soc.*, 2008, **130**, 14054.

28 J. Liu, P. Ruffieux, X. Feng, K. Müllen and R. Fasel, *Chem. Commun.*, 2014, **50**, 11200.

29 A. Wiengarten, K. Seufert, W. Auwärter, D. Ecija, K. Diller, F. Allegretti, F. Bischoff, S. Fischer, D. A. Duncan, A. C. Papageorgiou, F. Klappenberger, R. G. Acres, T. H. Ngo and J. V. Barth, *J. Am. Chem. Soc.*, 2014, **136**, 9346.